29th Congress of the International Council
of the Aeronautical Sciences
St. Petersburg, Russia; September 7–12, 2014

BOOST-PHASE MISSILE ATTITUDE CONTROLLER DESIGN USING HIGHER-ORDER SLIDING MODES

Yongwoo Lee[*], **Youdan Kim**[*], **Gwanyoung Moon**[**], **Byung-Eul Jun**[**]
[*]**Seoul National University, Seoul, 151-744, Republic of Korea,**
[**]**Agency for Defense Development, Daejeon, Republic of Korea**

Keywords: *Missile, Attitude Control, Boost-phase, Higher-order Sliding Mode Control*

Abstract

A higher-order sliding mode controller is proposed for integrated roll, pitch, and yaw attitude control of a velocity-varying skid-to-turn missile. For a system to be controlled, a missile model accompanying nonlinearly coupled aerodynamics is considered. To cope with the coupling effects between control input channels as well as nonlinearities, modeling for the aerodynamic effect is conducted based on the experimental aerodynamic coefficients using first-order taylor expansion. The resulting model is inherited in the govern equation for the rotational maneuver of the missile. Multiple sliding surfaces are designed and used simultaneously for the integrated control of the roll, pitch, and yaw angles. In particular, three sliding surfaces based on the attitude errors are used to take into account the rapid parameter variation as well as uncertainties which are arising during the boost-phase. The second-order sliding mode control scheme is also used to generate the control input, and stabilizing input for the general second-order sliding surface is applied by using a virtual input structure indirectly. Numerical simulation involving uncertainties is carried out to demonstrate the performance of the proposed controller.

1 Introduction

Recent progress of the high performance missiles has accelerated the development of the rapidly-maneuvering missile system, and lots of research on the missile control have been performed as in [1]-[7]. However, most of the missile autopilot have been designed on the assumption that the missile flies at constant speed, which enables the linearization and simple design of the controller. [1] This approach cannot be applied when the system to be controlled is under rapid parameter transition, for example, boost-phase. Indeed, this approach is not robust with respect to the rapidly-varying parameters. Therefore, robust nonlinear control method is required to design a controller under those conditions and nonlinear characteristics.

Attitude control of the boost-phase missile has been studied for some missile platforms such as the kinetic energy missile [2], high angle-of-attack missile [3], and vertical launch anti-submarine missile [4], which is controlled by both aerodynamic fin and thrusters. In Ref. [4], a robust attitude controller using quaternion feedback is proposed for the thrust vector control. None of those works, however, are focused on the three-dimensional attitude control of a fin-controlled missile during the boost-phase. Higher-order sliding mode control (SMC) is a nonlinear control scheme for a system with relative degree $r > 2$. As conventional SMC, it is robust to uncertainties and has also been applied for the control of missiles. [5]-[7]

In this study, an attitude controller based on the higher-order sliding mode control scheme is proposed for a tail-controlled skit-to-turn missiles to achieve immediate attitude control during the boost-phase. As a system to be controlled, a six degrees-of-freedom missile model involving nonlinear aerodynamics and cross-coupling ef-

fects between control input channels is considered. Mathematical modeling for the aerodynamic effect is conducted by using taylor-series expansion, and the resulting model is inherited in the equations of motion. To demonstrate the performance of the proposed attitude controller, numerical simulation involving uncertainties is performed for the velocity-varying missile. The rest of this paper is organized as follows. Section II is devoted to problem formulation, and Sec. III describes the controller design. Numerical simulation results are given in Sec. IV, and concluding remarks are provided in Sec. V.

2 Perliminaries

2.1 Problem Statement

The attitude control problem is defined as making the attitude of the missile to follow the commanded attitude, denoted as ϕ_c θ_c, and ψ_c with proper control inputs. Note that the states ϕ, θ, and ψ, representing roll, pitch, and yaw angle, with respect to the inertial coordinate is defined as the 'attitude'. The 'Euler equation' relates the angular velocity with respect to the body-fixed frame to the attitude-rate with respect to the inertial coordinate as follows

$$\begin{bmatrix} \dot{\phi} \\ \dot{\theta} \\ \dot{\psi} \end{bmatrix} = \begin{bmatrix} 1 & \sin\phi\tan\theta & \cos\phi\tan\theta \\ 0 & \cos\phi & -\sin\phi \\ 0 & \sin\phi\sec\theta & \cos\phi\sec\theta \end{bmatrix} \begin{bmatrix} p \\ q \\ r \end{bmatrix} \quad (1)$$

Under the small-angle assumption, time derivatives of those attitudes may be simplified as

$$\begin{bmatrix} \dot{\phi} \\ \dot{\theta} \\ \dot{\psi} \end{bmatrix} = \begin{bmatrix} p \\ q \\ r \end{bmatrix} \quad (2)$$

where p, q, and r represent roll-rate, pitch-rate, and yaw-rate, respectively. Similarly, control inputs are defined as δ_r, δ_p, and δ_y, representing roll, pitch, and yaw fin(surface) deflection angles, respectively.

2.2 Equations of Motions

In this study, rotational dynamics of the missiles is considered. Let us consider following equa-

tions of motions for rotational maneuver of symmetric cruciform missiles.[8]

$$\dot{p} = \frac{QSdC_l}{I_{xx}} - \frac{\dot{I}_{xx}}{I_{xx}}p \quad (3)$$

$$\dot{q} = \frac{(I_{zz} - I_{xx})pr}{I_{yy}} + \frac{QSdC_m}{I_{yy}} - \frac{\dot{I}_{yy}}{I_{yy}}q \quad (4)$$

$$\dot{r} = \frac{(I_{xx} - I_{yy})pr}{I_{zz}} + \frac{QSdC_n}{I_{zz}} - \frac{\dot{I}_{zz}}{I_{zz}}r \quad (5)$$

where (I_{xx}, I_{yy}, I_{zz}) are moments of inertia, Q, S, and d correspond to dynamic pressure, reference surface, and reference length, respectively, and C_l, C_m, and C_n represent nondimensionalized aerodynamic coefficients for roll, pitch, and yaw moments, respectively. In addition, time-derivatives of the moments of inertia ($\dot{I}_{xx}$, $\dot{I}_{yy}$, and $\dot{I}_{zz}$) are considered, in this study.

2.3 Aerodynamical Model

Roll, pitch, and yaw moment coefficients include the complex aerodynamic effect generated by airflows around the missile. The coefficients are usually experimentally obtained, and can be modeled as a function of several parameters as follows

$$C_i = f(M, h, \alpha, \beta, \delta_r, \delta_p, \delta_y), \ i = l, m, n \quad (6)$$

where M, α, and β represent Mach number, angle of attack, and sideslip angle, respectively. Every control input is considered as an argument of the function C_i as shown in Eq. (6), because there exist cross-coupling effects between input channels. Figure 1 shows the moment coefficients used in this study. The coefficients C_l, C_m, and C_n are evaluated at $h = 2,000m$, $M = 1.6$, $\beta = 0°$, and $\delta_r = \delta_p = \delta_y = 0$, and its magnitude and α_T, total angle of attack, is normalized by the maximum of each paramter. It is shown that the slope of the C_m varies, and even its sign alters as α_T changes and, C_n curve shows severe nonlinearity. Those nonzero moment coefficients, which have nonlinearities, are generated regardless of the control inputs that are set to zero, and this indicates that the attitude control should be made in an integrated manner. Figure 1

illustrates the aerodynamic moment coefficients at a constant speed, though, the aerodynamic effect changes as its speed varies, and the curve changes accordingly. Because the speed of the missile changes, the curves can be interpreted as time-varying function, and its variation becomes more complicated when the speed is rapidly accelerated during the boost-phase. Thus, a robust nonlinear control method is required to make the missile track the attitude command appropriately.
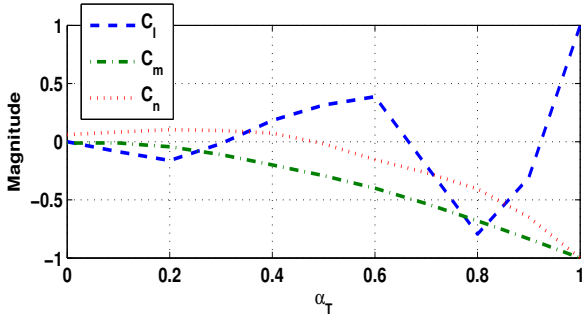

Fig. 1 Normalized C_l, C_m, and C_n ($M = 1.6$)

2.4 Mathematical Modeling of Moment Coefficients

The effects of the control surfaces can be modeled using first-order taylor expansion as follows.

$$C_l = C_{l_0} + C_{l_{\delta_r}}\delta_r + C_{l_{\delta_p}}\delta_p + C_{l_{\delta_y}}\delta_y \qquad (7)$$

$$C_m = C_{m_0} + C_{m_{\delta_r}}\delta_r + C_{m_{\delta_p}}\delta_p + C_{m_{\delta_y}}\delta_y \qquad (8)$$

$$C_n = C_{n_0} + C_{n_{\delta_r}}\delta_r + C_{n_{\delta_p}}\delta_p + C_{n_{\delta_y}}\delta_y \qquad (9)$$

where subscript 0 refers to aerodynamics that is not affected by the control surfaces, and the coefficients with subscripts δ_i, $i = r$, p, y, represent the aerodynamic effect generated by the control surfaces. In this study, aerodynamic database based on experimental data provides the aerodynamic coefficients at each time-step, and the coefficients appear in the right-hand-side of the Eqs. (7)-(9) are computed by the finite-difference method based on those data.

2.5 Input-affine Form

The equations of motion in Eqs. (3)-(5) does not show the effect of the control input explicitly. An input-affine model, which describes how the control input is reflected in the rotational maneuver, can be obtained by using the mathematical model given in Eqs. (7)-(9). Substituting Eqs. (7)-(9) into Eqs. (3)-(5) gives

$$\dot{p} = \frac{QSdC_l}{I_{xx}} - \frac{\dot{I}_{xx}}{I_{xx}}p \qquad (10)$$

$$= \frac{QSdC_{l_0}}{I_{xx}} - \frac{\dot{I}_{xx}}{I_{xx}}p$$

$$+ \frac{QSd(C_{l_{\delta_r}}\delta_r + C_{l_{\delta_p}}\delta_p + C_{l_{\delta_y}}\delta_y)}{I_{xx}} \qquad (11)$$

$$= L_0 + L_r\delta_r + L_p\delta_p + L_y\delta_y \qquad (12)$$

$$\dot{q} = \frac{(I_{yy} - I_{xx})pr}{I_{zz}} + \frac{QSdC_m}{I_{zz}} - \frac{\dot{I}_{zz}}{I_{zz}}q \qquad (13)$$

$$= \frac{(I_{yy} - I_{xx})pr}{I_{zz}} + \frac{QSdC_{m_0}}{I_{zz}} - \frac{\dot{I}_{zz}}{I_{zz}}q$$

$$+ \frac{QSd(C_{m_{\delta_r}}\delta_r + C_{m_{\delta_p}}\delta_p + C_{m_{\delta_y}}\delta_y)}{I_{zz}} \qquad (14)$$

$$= M_0 + M_r\delta_r + M_p\delta_p + M_y\delta_y \qquad (15)$$

$$\dot{r} = \frac{(I_{xx} - I_{zz})pr}{I_{yy}} + \frac{QSdC_{n_0}}{I_{yy}} - \frac{\dot{I}_{yy}}{I_{yy}}r$$

$$+ \frac{QSd(C_{n_{\delta_r}}\delta_r + C_{n_{\delta_p}}\delta_p + C_{n_{\delta_y}}\delta_y)}{I_{yy}} \qquad (16)$$

$$= N_0 + N_r\delta_r + N_p\delta_p + N_y\delta_y \qquad (17)$$

where

$$L_0 = \frac{QSdC_{l_0}}{I_{xx}} - \frac{\dot{I}_{xx}}{I_{xx}}p, \quad L_r = \frac{QSdC_{l_{\delta_r}}}{I_{xx}} \qquad (18)$$

$$L_p = \frac{QSdC_{l_{\delta_p}}}{I_{xx}}, \quad L_y = \frac{QSdC_{l_{\delta_y}}}{I_{xx}} \qquad (19)$$

$$M_0 = \frac{(I_{yy} - I_{xx})pr}{I_{zz}} + \frac{QSdC_{l_0}}{I_{xx}} - \frac{\dot{I}_{zz}}{I_{zz}}q, \qquad (20)$$

$$M_r = \frac{QSdC_{l_{\delta_r}}}{I_{zz}} \qquad (21)$$

$$M_p = \frac{QSdC_{l_{\delta_p}}}{I_{zz}}, \quad M_y = \frac{QSdC_{l_{\delta_y}}}{I_{zz}} \qquad (22)$$

$$N_0 = \frac{QSdC_{n_0}}{I_{xx}} - \frac{\dot{I}_{xx}}{I_{yy}}r, \quad N_r = \frac{QSdC_{n_{\delta_r}}}{I_{yy}} \qquad (23)$$

$$N_p = \frac{QSdC_{n_{\delta_p}}}{I_{yy}}, \quad N_y = \frac{QSdC_{n_{\delta_y}}}{I_{yy}} \qquad (24)$$

Finally, the rotational motion of the missile can be expressed in an input-affine form as follows

$$
\begin{bmatrix} \dot{p} \\ \dot{q} \\ \dot{r} \end{bmatrix} = \begin{bmatrix} L_0 \\ M_0 \\ N_0 \end{bmatrix} + \begin{bmatrix} L_r & L_p & L_y \\ M_r & M_p & M_y \\ N_r & N_p & N_y \end{bmatrix} \begin{bmatrix} \delta_r \\ \delta_p \\ \delta_y \end{bmatrix} + \begin{bmatrix} w_\phi \\ w_\theta \\ w_\psi \end{bmatrix}
$$

$$(25)$$

where w_ϕ, w_θ, and w_ψ are supplemented to represent the bundle of unmodeled dynamics and disturbance.

3 Attitude Controller Design

3.1 Sliding Surface

To apply the SMC for designing attitude controller, sliding surfaces should be defined in advance. The attitude tracking objective can be achieved by stabilizing the error between the current attitude angle and the commanded one. The attitude errors can be defined as

$$e_\phi = \phi - \phi_c \qquad (26)$$

$$e_\theta = \theta - \theta_c \qquad (27)$$

$$e_\psi = \psi - \psi_c \qquad (28)$$

Note that the attitude is composed of the three components to be controlled and three independent control inputs are available, and therefore three independent sliding surfaces can be used. Let us choose the sliding surfaces as follows

$$\sigma_\phi = \left(\frac{d}{dt} + \lambda_\phi \right) \int_0^T e_\phi dt \qquad (29)$$

$$\sigma_\theta = \left(\frac{d}{dt} + \lambda_\theta \right) \int_0^T e_\theta dt \qquad (30)$$

$$\sigma_\psi = \left(\frac{d}{dt} + \lambda_\psi \right) \int_0^T e_\psi dt \qquad (31)$$

where λ_i's are positive real constants.

3.2 Second-order Sliding Mode Controller Design

In this section, the attitude control input is generated by using the SMC. Note that the relative degree of both the attitude dynamics and the sliding surfaces given in Eqs. (29)-(31) is identical,

and therefore the second-order SMC is applicable. General form of the second-order sliding surface is given as follows.

$$\ddot{\sigma} = h(\sigma, \dot{\sigma}, t) + k(t)u_{(\sigma)}, \quad k(t) > 0 \qquad (32)$$

where $k_m < k(t) < k_M$, and $|h(\sigma, \dot{\sigma}, t)| \leq C$ for some k_m, K_M, and C. A control input that stabilizes $\ddot{\sigma}$, $\dot{\sigma}$, and σ to zero can be designed as follows [9]

$$u(\sigma_i) = -\alpha_i \frac{\dot{\sigma}_i + \beta_i |\sigma_i|^{1/2} sgn(\sigma_i)}{||\dot{\sigma}_i| + \beta_i |\sigma_i|^{1/2} sign(\sigma)|} \qquad (33)$$

where α_i, and β_i are design parameters that satisfy

$$\alpha_i, \beta_i > 0 \qquad (34)$$

$$\alpha_i k_m - C > \frac{\beta^2}{2} \qquad (35)$$

The strength of the higher-order SMC is that the sliding surface converges to zero in a smooth fashion. Therefore, state responses will be reached in steady values, because the control input forces all of its time-derivatives converge to zero. A drawback of this approach that it is not straightforward to estimate the minimum of the function $h(\dot{\sigma}, \sigma, t)$ and $k(t)$, represented by C and k_m, respectively. The estimation should be performed in a conservative manner to guarantee that the bounds of those variables are not underestimated nor exaggerated. This practice, however, could deteriorate the control performance if the estimated bounds are inaccurate. To avoid such miscalculation, an alternative approach is used in this study. Instead of directly applying the control input, let us consider a virtual system as follows

$$\ddot{\sigma} = v \qquad (36)$$

Note that the original system given in Eq. (32) can be transformed into the virtual system in Eq. (36) with an augmented control input defined as

$$u_\sigma = k(t)^{-1} \{-h(\sigma, \dot{\sigma}, t) + v\} \qquad (37)$$

where

$$v = -\alpha_i \frac{\dot{\sigma}_i + \beta_i |\sigma_i|^{1/2} sgn(\sigma_i)}{|\dot{\sigma}_i| + \beta_i |\sigma_i|^{1/2}} \qquad (38)$$

Note that $k(t)^{-1}$ always exists, because $0 < k_m < k(t) < k_M$. The input reformulates the system to be a double-integrator system as in Eq. (36), which is identical to Eq. (32) with parameters $h(\sigma, \dot{\sigma}, t) = 0$, and $k(t) = 1$. With those values, the requirement for the design parameters imposed in Eq. (35) becomes

$$\alpha_i > \frac{\beta_i^2}{2} \tag{39}$$

The new condition in Eq. (39) makes the design procedure of the control input v less complicated. The actual fin-deflection command u is generated using Eq. (37), (38) and Eq. (39). By differentiating Eqs. (29)-(31) with respect to time twice after substituting Eqs. (7)-(9) into Eqs. (3)-(5), we have

$$\ddot{\sigma}_\phi = \ddot{e}_\phi + \lambda_\phi \dot{e}_\phi \tag{40}$$
$$= \ddot{\phi} - \ddot{\phi}_c + \lambda_\phi(\dot{\phi} - \dot{\phi}_c) \tag{41}$$
$$= L_0 + L_r \delta_r + L_p \delta_p + L_y \delta_y$$
$$- \dot{\phi}_c + \lambda_\phi(\phi - \phi_c) \tag{42}$$

$$\ddot{\sigma}_\theta = \ddot{e}_\theta + \lambda_\theta e_\theta \tag{43}$$
$$= \ddot{\theta} - \ddot{\theta}_c + \lambda_\theta(\dot{\theta} - \dot{\theta}_c) \tag{44}$$
$$= M_0 + M_r \delta_r + M_p \delta_p + M_y \delta_y$$
$$- \ddot{\theta}_c + \lambda_\theta(\dot{\theta} - \dot{\theta}_c) \tag{45}$$
$$\ddot{\sigma}_\psi = \ddot{e}_\psi + \lambda_\psi \dot{e}_\psi \tag{46}$$
$$= \ddot{\psi} - \ddot{\psi}_c + \lambda_\psi(\dot{\psi} - \dot{\psi}_c) \tag{47}$$
$$= N_0 + N_r \delta_r + N_p \delta_p + N_y \delta_y$$
$$- \ddot{\psi}_c + \lambda_\psi(\dot{\psi} - \dot{\psi}_c) \tag{48}$$

Re-arranging Eqs. (40)-(48) into a matrix form, the sliding surfaces can be expressed as follows

$$\begin{bmatrix} \ddot{\sigma}_\phi \\ \ddot{\sigma}_\theta \\ \ddot{\sigma}_\psi \end{bmatrix} = H + Ku \tag{49}$$

where

$$H = \begin{bmatrix} L_0 - \dot{\phi}_c + \lambda_\phi(\phi - \phi_c) \\ M_0 - \dot{\theta}_c + \lambda_\theta(\theta - \theta_c) \\ N_0 - \dot{\psi}_c + \lambda_\psi(\psi - \psi_c) \end{bmatrix} \tag{50}$$

$$K = \begin{bmatrix} L_r & L_p & L_y \\ M_r & M_p & M_y \\ N_r & N_p & N_y \end{bmatrix}, \quad u = \begin{bmatrix} \delta_r \\ \delta_p \\ \delta_y \end{bmatrix} \tag{51}$$

Note that K^{-1} always exists by the intentional configuration design of the missile control surface. Observing the structural similarity between Eq. (32) and Eq. (49), and utilizing the control input proposed in (37), the fin deflection command can be obtained as follows

$$u = -B^{-1}(H + v) \tag{52}$$

where

$$v = \begin{bmatrix} v_\phi \\ v_\theta \\ v_\psi \end{bmatrix}$$
$$= \begin{bmatrix} -\alpha_\phi sign(\dot{\sigma}_\phi + \beta_\phi|\sigma_\phi|^{1/2} sign(\sigma_\phi) \\ -\alpha_\theta sign(\dot{\sigma}_\theta + \beta_\theta|\sigma_\theta|^{1/2} sign(\sigma_\theta) \\ -\alpha_\psi sign(\dot{\sigma}_\psi + \beta_\psi|\sigma_\psi|^{1/2} sign(\sigma_\psi) \end{bmatrix} \tag{53}$$

Finally, integrated attitude control can be conducted by the command of Eq. (52), which stabilizes the attitude error in roll, pitch, and yaw channels simultaneously. Architecture of the proposed attitude controller is shown in Fig. 2. The
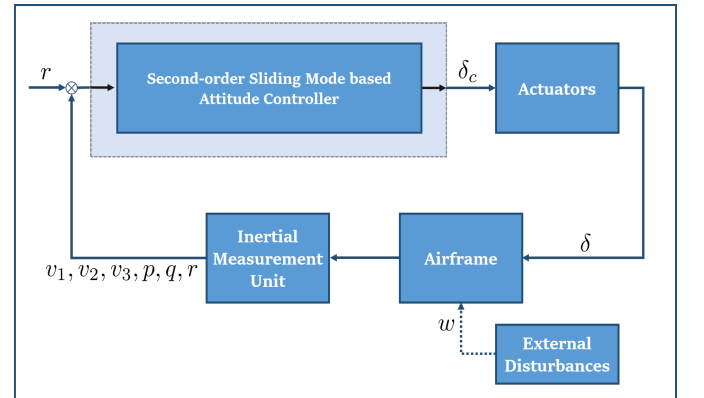

Fig. 2 Block-diagram of the attitude controller

fin-deflection command $\delta_{r_c}, \delta_{p_c}$, and δ_{y_c} generated by the proposed attitude controller is transferred to actuators, then the missile dynamics is affected by the fin-deflection δ_r, δ_p, and δ_y achieved through the actuator units. The feedback control is performed by providing the attitude and angular velocity, which are measured by the inertial measurement unit, to the attitude controller.

Table 1 Simulation Parameters

Symbol	Description	Value
$[\phi,\ \theta,\ \psi]_{(0)}$	Initial Attitude	$[0°, 90°, 0°]$
$[\phi,\ \theta,\ \psi]_{(c)}$	Commanded Attitude	$[0°,\ 0°, 0°]$
$V_T(0)$	Initial Total Velocity	25m/s

4   Numerical Simulation

Numerical simulation is carried out to demonstrate the performance and robustness of the proposed controller. For the actuator unit, a following stable second-order dynamics is considered

$$\frac{\delta}{\delta_c} = \frac{\omega_n^2}{s^2 + 2\zeta\omega_n s + \omega_n^2} \qquad (54)$$

where δ, δ_c, ω_n, and ζ are actual fin-deflection, commanded fin-deflection, natural frequency, and damping ratio, respectively. Nonlinear characteristics include following fin-deflection rate limit C_δ and the deflection angle limit δ_M

$$|\dot{\delta}| \leq C_\delta \qquad (55)$$
$$|\delta| \leq \delta_M \qquad (56)$$

4.1   Simulation Scenario

Initial conditions and commanded attitude are summarized in Table 1, and the following model uncertainty is considered.

$$w = k_d \begin{bmatrix} sin(1.8\pi t) & 0 & 0 \\ 0 & sin(2\pi t) & 0 \\ 0 & 0 & sin(2.1\pi t) \end{bmatrix} H \qquad (57)$$

The matrix w represents the unmodeled dynamics and disturbances generated by internal and external uncertainties. Both the nominal system ($||w||_2 = 0$) and disturbed system ($||w||_2 \neq 0$) are simulated to recognize the effectiveness of the proposed controller; the former is to demonstrate the performance of the controller under ideal circumstances, whereas the latter is to examine its robustness with respect to various uncertainties.
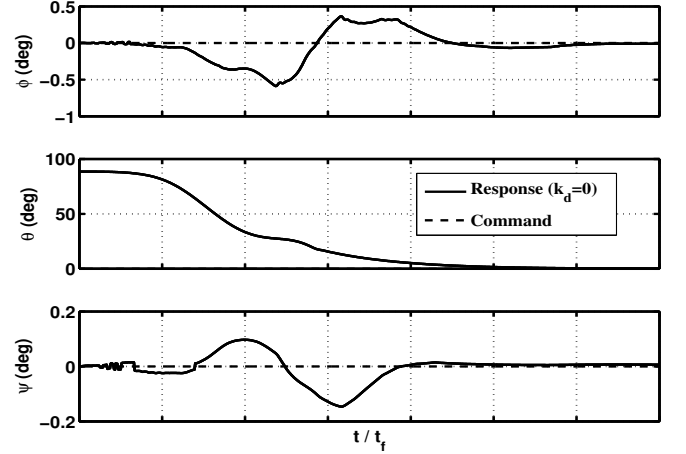
Fig. 3 Nominal case : attitude response
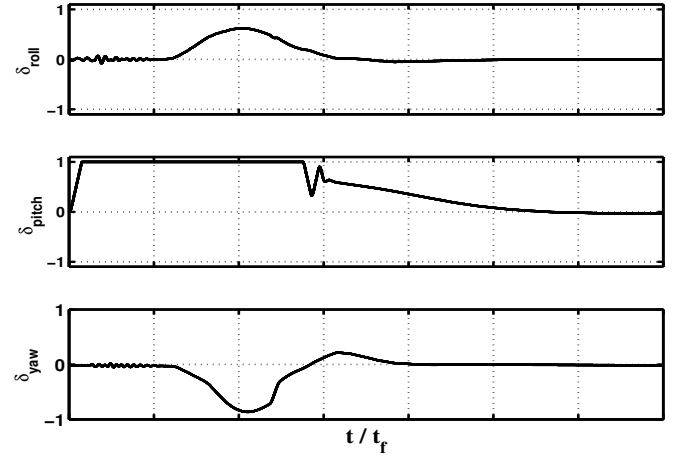
Fig. 4 Nominal case : control history
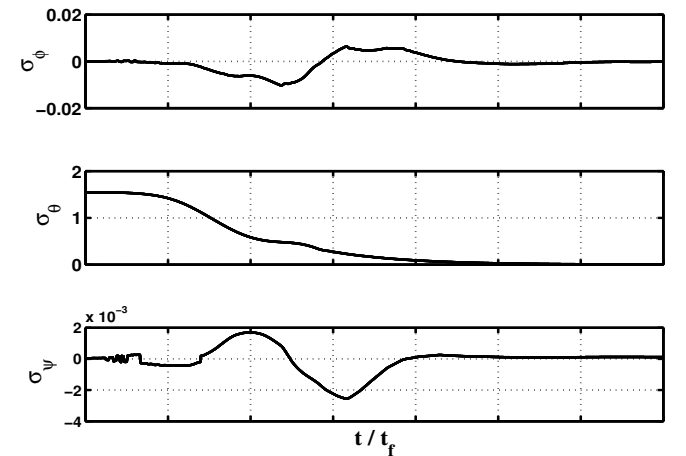
Fig. 5 Nominal case : sliding surfaces response

4.2 Nominal system

Figures 3 - 5 show the simulation results for the nominal case. Figure 3 shows that desired attitude is achieved with acceptable error less than 0.2°. Control input histories are depicted in Fig. 4. The roll, pitch, yaw fin-deflections are normalized by their maximum value, which are represented as δ_{roll}, δ_{pitch}, and δ_{yaw}, respectively. The horizontal axes, in addition, is normalized by the final time t_f. Pitch channel control input δ_{pitch} is saturated in the transient phase, but converges to zero as the pitch attitude tracks the command. Control inputs for other channels, δ_{roll}, and δ_{yaw} also converge to zero as the attitude error decreases. Figure 5 shows the time responses of the sliding surfaces, and similar trend to attitude responses can be observed. From the simulation results, it can be concluded that the controller exhibits good performance for the system without disturbance.

4.3 Monte-Carlo Simulation with Disturbed System

The performance of the controller is examined under various external environment modeled as

$$w = N(0, \sigma^2) \tag{58}$$
$$k_d \in [0, 0.5] \tag{59}$$

To acquire the reliability, furthermore, the Monte-Carlo simulation is performed for $N = 100$ times using k_d within the given range. Figure 6 shows the time histories of the attitude. The attitude error growth associated with increase of the parameter k_d supports the effect of the uncertainty on the control performance. The attitude at the final time, however, satisfies the commanded value with negligible amount of error. The control histories are shown in Fig. 7, and the sliding surfaces are depicted in Fig. 8. As the uncertainty has been elevated, the control inputs and the sliding surfaces have also been deviated from the ideal response, but the general tendency of the convergence is maintained for all cases. Figure 9 shows the time histories of the velocity. The longitudinal speed v_1 rapidly increases the force provided by the thrust during the boosting phase.

From the results, it can be stated that the controller is robust with respect to the uncertainty described as in Eqs. (57)-(59).
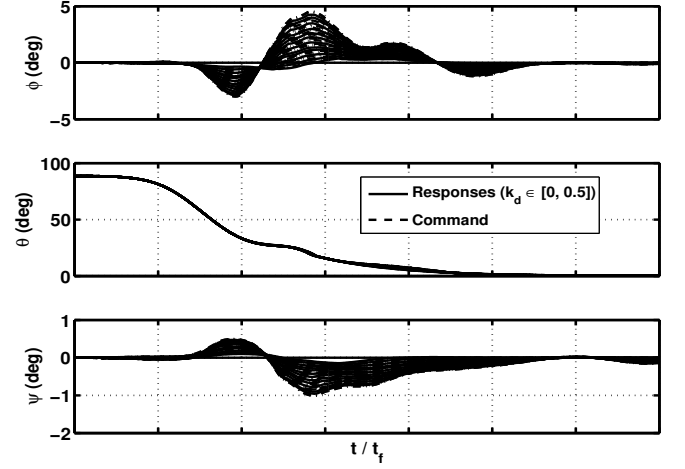

Fig. 6 Disturbed case : attitude responses
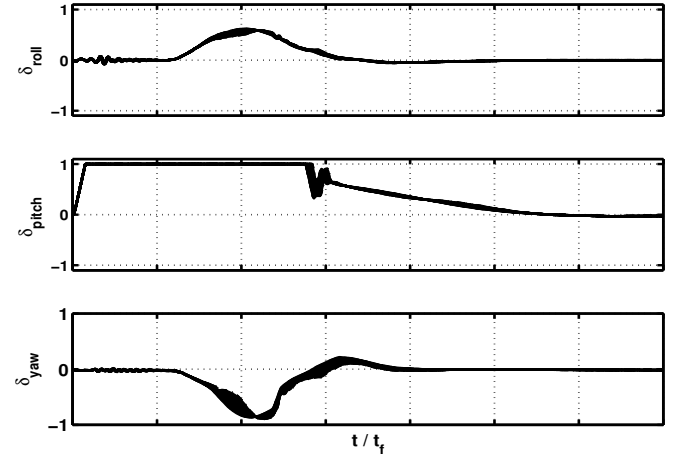
Fig. 7 Disturbed case : control histories
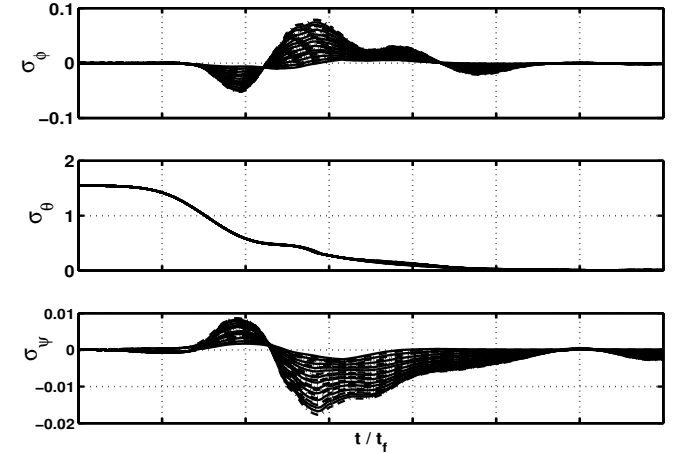
Fig. 8 Disturbed case : sliding surfaces responses

**YONGWOO LEE*, YOUDAN KIM*, GWANYOUNG MOON**, BYUNG-EUL JUN**
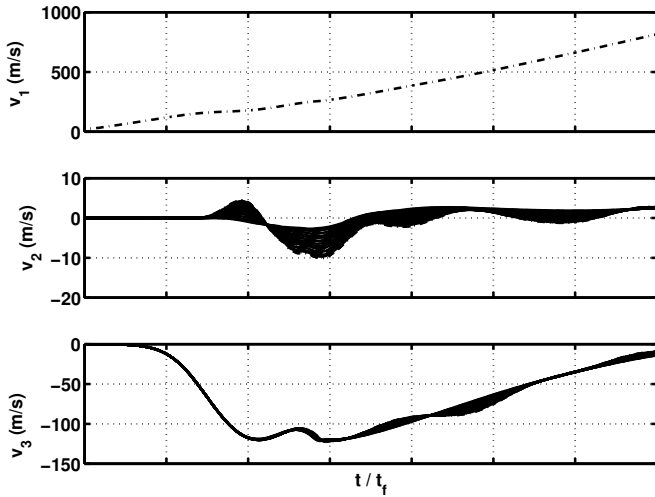
Fig. 9 Disturbed case : velocity responses

5 Conclusion

Higher-order sliding mode based attitude controller using multiple sliding surfaces is proposed for the missile with rapidly time-varying dynamic and aerodynamic characteristics. The control input vector was generated by using a virtual structure which transforms the system into a double-integrator system. Multiple sliding surfaces were considered simultaneously for the integrated roll, pitch, and yaw attitude control. Numerical simulation was conducted and the results exploited noticeable performance and robustness to uncertainties with satisfactory attitude control results.

References

[1] H. Buschek, "Full Envelope Missile Autopilot Design Using Gain Scheduled Robust Control," *Journal of Guidance, Control, and Dynamics*, Vol. 22, No. 1, 1999, pp. 115-122.

[2] H. J. Gratt, and W. L. McCowan, "Feedback Linearization Autopilot Design for the Advanced Kinetic Energy Missile Boost Phase," *Journal of Guidance, Control and Dynamics,* Vol. 18, No. 5, 1995, pp. 945-950.

[3] Innocenti, M., "A Sliding Mode Missile Pitch Autopilot Synthesis for High Angle of Attack Maneuvering," *IEEE Transactions on Control System Technology*, Vol. 6, No. 3, 1998, pp. 359-371.

[4] C. Song, S.-J. Kim, S.-H. Kim, and H. S. Nam, "Robust Control of the Missile Attitude based on Quaternion Feedback," *Control Engineering Practice*, Vol. 14, No. 7, 2006, pp. 811-818.

[5] A. Levant, A. Pridor, R. Gitizadeh, I. Yaesh, and J. Z. Ben-Asher, "Aircraft Pitch Control via Second-Order Sliding Technique," *Journal of Guidance, Control, and Dynamics*, Vol. 23, No. 4, 2000, pp. 586-594.

[6] Y. B. Shtessel, and C. H. Tournes, "Integrated Higher-order Sliding Mode Guidance and Autopilot for Dual Control Missiles," *Journal of Guidance, Control, and Dynamics*, Vol. 32, No.1, 2009, pp. 79-94.

[7] Y. Shtessel, I. Shkolnikov, and A. Levant, "Smooth Second Order Sliding Modes: Missile Guidance Application," *Automatica*, Vol. 43, No. 8, 2007, pp. 1470-1476.

[8] J. H. Blakelock, *Automatic Control of Aircraft and Missile,* New York, NY, Wiley, 1991.

[9] A. Levant, "Higher-Order Sliding Modes, Differentiation and Output-Feedback Control," *International Journal of Control*, Vol. 76, Nos. 9-10, 2003, pp. 924-941.

Contact Author Email Address

- Yongwoo Lee (mailto:leeyw@snu.ac.kr)
- Youdan Kim (corresponding author, mailto:ydkim@snu.ac.kr)

Acknowledgement

Copyright Statement